INFECTION AND IMMUNITY, Aug. 2011, p. 3117–3130 Vol. 79, No. 8
0019-9567/11/$12.00 doi:10.1128/IAI.05136-11

The Hybrid Histidine Kinase Hk1 Is Part of a Two-Component System That Is Essential for Survival of *Borrelia burgdorferi* in Feeding *Ixodes scapularis* Ticks▽†

Melissa J. Caimano,[1]* Melisha R. Kenedy,[2]‡ Toru Kairu,[3]‡ Daniel C. Desrosiers,[1] Michael Harman,[1] Star Dunham-Ems,[1] Darrin R. Akins,[2] Utpal Pal,[3] and Justin D. Radolf[1,4]

Departments of Medicine[1] and Genetics and Developmental Biology,[4] University of Connecticut Health Center, Farmington, Connecticut 06030; Department of Microbiology and Immunology, University of Oklahoma Health Sciences Center, Oklahoma City, Oklahoma 73104[2]; and Department of Veterinary Medicine, University of Maryland, College Park, Maryland 20742[3]

Received 27 March 2011/Returned for modification 23 April 2011/Accepted 12 May 2011

Two-component systems (TCS) are principal mechanisms by which bacteria adapt to their surroundings. *Borrelia burgdorferi* encodes only two TCS. One is comprised of a histidine kinase, Hk2, and the response regulator Rrp2. While the contribution of Hk2 remains unclear, Rrp2 is part of a regulatory pathway involving the spirochete's alternate sigma factors, RpoN and RpoS. Genes within the Rrp2/RpoN/RpoS regulon function to promote tick transmission and early infection. The other TCS consists of a hybrid histidine kinase, Hk1, and the response regulator Rrp1. Hk1 is composed of two periplasmic sensor domains (D1 and D2), followed by conserved cytoplasmic histidine kinase core, REC, and Hpt domains. In addition to its REC domain, Rrp1 contains a GGDEF motif characteristic of diguanylate cyclases. To investigate the role of Hk1 during the enzootic cycle, we inactivated this gene in two virulent backgrounds. Extensive characterization of the resulting mutants revealed a dramatic phenotype whereby Hk1-deficient spirochetes are virulent in mice and able to migrate out of the bite site during feeding but are killed within the midgut following acquisition. We hypothesize that the phosphorelay between Hk1 and Rrp1 is initiated by the binding of feeding-specific ligand(s) to Hk1 sensor domain D1 and/or D2. Once activated, Rrp1 directs the synthesis of cyclic dimeric GMP (c-di-GMP), which, in turn, modulates the expression and/or activity of gene products required for survival within feeding ticks. In contrast to the Rrp2/RpoN/RpoS pathway, which is active only within feeding nymphs, the Hk1/Rrp1 TCS is essential for survival during both larval and nymphal blood meals.

Two-component signal transduction systems (TCSs) are principal mechanisms by which bacteria survey and adapt to perturbations in their surroundings (29, 44). Typically, TCSs are composed of sensor histidine kinase (HK) and response regulator (RR) components, with the genes encoding a particular TCS frequently being cotranscribed (25, 29). The majority of TCS HKs consist of a variable extracytoplasmic sensor domain and conserved cytoplasmic kinase core containing catalytic ATP-binding (CA) and dimerization/histidine phosphotransfer (DHp) domains (29). RR proteins typically are comprised of a conserved receiver (REC) domain and an effector domain (26, 29). In its simplest form, regulation via TCSs begins with the binding of a specific ligand by the HK sensor domain, which in turn induces a conformation change promoting autophosphorylation of a His residue within the kinase core (29). The cognate RR then catalyzes the transfer of the phosphoryl group from the phosphorylated His (His~P) to an Asp residue within its own REC domain (29). Once activated, the RR effector domain elicits an appropriate response, typically by altering transcription of specific genes or allosteric regulation of target proteins (26). Although examples of cross talk have been reported, bacteria have evolved multiple mechanisms to prevent inadvertent signaling between unrelated HK and RR components (69).

The genome of *Borrelia burgdorferi*, the Lyme disease spirochete, encodes two TCSs in addition to the CheA and CheY orthologs associated with chemotaxis (24, 31). One consists of a sensor histidine kinase (Hk2/BB0764) and response regulator (Rrp2/BB0763), both of which are predicted to localize to the cytoplasm. Although Hk2 was widely presumed to be the cognate HK for Rrp2, Xu et al. (86) recently demonstrated that the high-energy, phosphoryl donor acetyl phosphate (acetyl~P) is capable of phosphorylating Rrp2 *in vitro* and, more importantly, that Hk2 is not required for activation of Rrp2 *in vivo*. Once activated, Rrp2~P acts as a transcriptional activator for the alternate sigma factor RpoN (6, 87), which in turn controls expression of the spirochete's other alternate sigma factor, RpoS (7, 20, 36, 52, 70). Genes within the Rrp2/RpoN/RpoS regulon promote tick-to-mammal transmission (30) and early murine infection (10, 20, 32, 68, 80, 83).

The other borrelial TCS is composed of a sensor histidine kinase (Hk1/BB0420) and response regulator (Rrp1/BB0419) (24). Hk1 consists of a periplasmic sensor domain flanked by two transmembrane helices followed by a histidine kinase core, REC, and previously unrecognized histidine-containing phosphotransfer (Hpt; described below) domains while Rrp1 con-

* Corresponding author. Mailing address: Department of Medicine, University of Connecticut Health Center, 263 Farmington Ave., Farmington, CT 06030-3715. Phone: (860) 679-8390. Fax: (860) 679-1358. E-mail: mcaima@up.uchc.edu.

‡ M.R.K. and T.K. contributed equally to this work.

† Supplemental material for this article may be found at http://iai.asm.org/.

▽ Published ahead of print on 23 May 2011.

TABLE 1. Bacterial strains used in these studies

Strain	Description	Reference or source
CE162	Wild-type virulent strain 297 parent	11
5A4 NP1	Wild-type virulent strain B31 parent	40
Bb508	CE162 transformed with pMC1389; strain 297 *hk1* mutant	This study
Bb807	CE162 transformed with pMC1389; strain 297 *hk1* mutant	This study
Bb1197	B31 5A4 NP transformed with pMC1389; strain B31 *hk1* mutant	This study
Bb914	CE162 cells containing P_{flaB}-*gfp* reporter inserted into cp26	16
Bb1152	Bb914 transformed with pMC1389; *hk1* mutant constitutively expressing GFP	This study
Bb1155	Bb914 transformed with pMC1389; *hk1* mutant constitutively expressing GFP	This study
Bb1363	Bb1197 complemented in *trans* with *hk1* contained a cp9-based shuttle vector	This study
Bb1367	Bb1197 complemented in *trans* with *hk1* contained a cp9-based shuttle vector	This study
5A13-Δrrp1	Strain B31 5A13 *rrp1* mutant	58

tains a REC domain as well as a GGDEF domain characteristic of diguanylate cyclases (27), the enzyme responsible for synthesis of the small nucleotide messenger bis-(3′-5′)-cyclic dimeric GMP (c-di-GMP) (59). Activation of Rrp1's diguanylate cyclase activity requires phosphorylation of its REC domain (59), presumably mediated by Hk1-dependent phosphorelay. Once produced, c-di-GMP induces a conformational change in one or more target proteins, altering their enzymatic activity or their ability to interact with DNA or other proteins (65). More recently, c-di-GMP also has been shown to directly alter gene expression via its interaction with the 5′ untranslated region of target mRNAs (45, 71). Evidence for a complete c-di-GMP signaling pathway in *B. burgdorferi* recently was confirmed by studies demonstrating that BB0363, an EAL domain-containing phosphodiesterase, specifically degrades c-di-GMP (76). In bacteria, c-di-GMP-mediated signaling has been associated with a wide range of adaptive processes, most notably the transition between planktonic and sessile lifestyles and biofilm formation (13, 34, 85).

Hk1 and Rrp1 are predicted to function cooperatively, and, as such, inactivation of either gene would result in a similar phenotype. Microarray analyses of a Δ*rrp1* mutant indentified 140 genes whose expression was influenced by this RR *in vitro* (58), several of which encode proteins whose annotated functions suggest a role in carbon metabolism, maintenance of the spirochete's cell envelope, and adaptation to the arthropod vector and/or mammalian host. However, because the background used to generate this Δ*rrp1* mutant was avirulent (58), the contribution of Rrp1 to virulence could not be determined. Therefore, to determine the role of the Hk1/Rrp1 TCS during the enzootic cycle, we sought to inactivate both genes within a virulent strain 297 background. While our attempts to isolate a strain 297 *rrp1* mutant were unsuccessful, we obtained multiple *hk1* mutants in strains 297 and B31 5A4 NP1. Extensive characterization of these mutants revealed a dramatic phenotype whereby Hk1-deficient spirochetes are fully virulent in mice and able to migrate into ticks during feeding but are killed within the midgut following acquisition. *trans*-Complementation restored the ability of the B31 *hk1* mutant to survive within both larvae and nymphs. Recently, studies by two independent laboratories demonstrated that *B. burgdorferi* lacking Rrp1 displays an identical survival defect (33a, 41a), establishing overwhelmingly that the protective function of Hk1 is mediated via phosphorelay. In contrast to Rrp2, which is active only during the nymphal blood meal (11, 49), the Hk1/Rrp1 TCS is required during both larval and nymphal life stages. Signaling via Hk1 appears to be induced by host- and/or tick-derived stimuli generated as part of the feeding process. The sensing of feeding-specific signals, encountered within the bite site and/or tick midgut, is presumably mediated by Hk1's D1 and D2 periplasmic sensor domains, both of which share structural similarities to bacterial extracellular solute-binding proteins (78).

MATERIALS AND METHODS

Bacterial strains and culture conditions. *B. burgdorferi* isolates used in these studies (Table 1) were cultivated in modified Barbour-Stoenner-Kelly medium (57) supplemented with 6% rabbit serum (Pel-Freeze Biologicals, Rogers, AK) (BSK-II). Strain 297 *hk1* mutants Bb508 and Bb807 were maintained under selection using streptomycin (50 μg/ml), while the strain B31 5A4 NP1 *hk1* mutant Bb1197 was maintained under selection using streptomycin (50 μg/ml) and kanamycin (400 μg/ml). *B. burgdorferi* isolates expressing a P_{flaB}-*gfp* reporter inserted into the 26-kb circular plasmid (cp26) were maintained under selection using gentamicin (50 μg/ml). The plasmid content of all isolates was monitored as previously described (18). Standard temperature shift experiments and growth curves were performed as previously described (11). To obtain organisms in a host-adapted state, spirochetes were cultivated in dialysis membrane chambers (DMCs) implanted into the peritoneal cavities of rats as previously described (1). *Escherichia coli* strains were maintained in Luria-Bertani broth (LB) (1% tryptone, 0.5% yeast extract, 1% NaCl) with the appropriate antibiotic. Selection was performed on LB agar plates (LB with 1.5% agar) supplemented with the appropriate antibiotic.

DNA manipulations and routine cloning. Routine molecular cloning and plasmid propagation were performed using *E. coli* Top10 cells (Invitrogen, Carlsbad, CA). Routine and high-fidelity PCR amplification reactions were performed using Choice *Taq* (Denville Scientific, Metuchen, NJ) and Takara ExTaq (Fisher Scientific, Pittsburgh, PA), respectively. Plasmid DNAs were purified from *E. coli* using Qiagen Midi and Spin Prep Kits (Valencia, CA). Nucleotide sequencing was performed by Agencourt Bioscience Corp. (Beverly, MA).

Bioinformatics. Routine and comparative sequence analyses were performed using MacVector (version 10.1; MacVector, Inc., Cary, NC). Conserved domain searches were performed using a conserved domains database (CDD) search either alone (http://www.ncbi.nlm.nih.gov/Structure/cdd/cdd.shtml) or within the NCBI Basic Local Alignment Search Tool (BLAST). Pairwise and multiple sequence alignments (PA and MSA, respectively) were performed using the ClustalW (version 1.83) (79) option within MacVector. Structural similarities and modeling were performed using Swiss-Model (http://swissmodel.expasy.org/) (2). The molecular viewer program PyMOL (www.pymol.org) (14) was used to generate the structural representations and calculate root mean square deviation (RMSD) values.

Generation and complementation of *B. burgdorferi hk1* mutants. A 4.9-kb region containing *hk1* and flanking sequences was amplified from strain 297 using primers ups.hk1-5′ and dwns.hk1-3′ (Table 2) and cloned into the pCR2.1-TOPO vector (Invitrogen). The resulting plasmid was digested with HpaI and ligated with a P_{flgB}-*aadA* cassette conferring resistance to spectinomycin (*E. coli*; 100 μg/ml) and streptomycin (*B. burgdorferi*; 50 μg/ml) (23), to yield pMC1389. The orientation of the *hk1* and *aadA* genes within pMC1389 was assessed by

TABLE 2. Oligonucleotide primers used in these studies

Primer[a]	Sequence (5′–3′)[b]	Purpose	Reference or source
hk1-F	CGTCAATTTATTTTCTAAGGATATTTTC	qRT-PCR	This work
hk1-R	TGCTTCGTCTTCAATTTCACT	qRT-PCR	This work
rrp1-F	AAGGTGCTTACGAGATTGAG	qRT-PCR	This work
rrp1-R	TCTGTGGAACTTCTTGAACTAA	qRT-PCR	This work
ups.hk1-5′	GGGTCCTGGAAGAATACCAGGTTG	Cloning and mutagenesis	This work
dwns.hk1-3′	GTGGGGAGAATCATCCACAATTAA	Cloning and mutagenesis	This work
hk1-KO-5′	CCCATTCAACATTTTTATCCAATTTT	Confirm insertion within *hk1*	This work
hk1-KO-3′	TGGACCAGCATCATCATTGCTTAGGTCTTTTG	Confirm insertion within *hk1*	This work
hk1-KO junc-5′	AGGTTAAAAAACGTTAACACCAT	Confirm complementation	This work
flgB-5′	GCG**CCATGG**TACCCGAGCTTCAAGGAAGA	Construction pSP1G	This work
gent-3′	GCG**CCATGG**TTAGGTGGCGGTACTTGGG	Construction pSP1G	This work
Hk1 compl-5′	GCG**GGATCC**GGGTCCTGGAAGAATACCAG	Complementation	This work
Hk1 compl-3′	GCG**CTGCAG**TTCCACTGCTAATATCTCTTATT	Complementation	This work
flaB-F	CTTTTCTCTGGTGAGGGAGCTC	qRT-PCR, qPCR	53
flaB-R	GCTCCTTCCTGTTGAACACCC	qRT-PCR, qPCR	53
flaB-Probe	CTTGAACCGGTGCAGCCTGAGCA	qRT-PCR, qPCR	53
nidogen-F	CCCCAGCCACAGAATACCAT	qPCR	81
nidogen-R	AAAGGCGCTACTGAGCCGA	qPCR	81
nidogen-probe	CCGGAACCTTCCCACCCAGC	qPCR	81

[a] F, forward; R, reverse.
[b] Restriction sites are in boldface.

PCR using primers ups.hk1-KO-5′ (where KO is knockout) and aadA-5′ and subsequently confirmed by sequencing. Competent CE162 cells were prepared as previously described (60) and electrotransformed with 15 to 20 μg of purified pMC1389. Streptomycin-resistant transformants were assessed for an insertion within *hk1* using primers hk1-KO-5′ and hk1-KO-3′. Two transformants (Bb508 and Bb807) derived from independent batches of CE162, each retaining a full plasmid complement, were selected for further analyses. A strain B31 *hk1* mutant (Bb1197) was generated by transforming competent 5A4 NP1 (40) with pMC1389 as described above.

Bb1197 was complemented with a wild-type copy of *hk1* inserted into pSP1G, a gentamicin-resistant derivative of pBSV2 (75). To modify pBSV2, the gentamicin resistance cassette was amplified from pSPCG (41) using primer flgB-5′ and primer gent-3′ and inserted into the NcoI site of pBSV2. The pBSV2 kanamycin resistance cassette was inactivated by digesting the vector with PvuI, which removed the *flgB* promoter and the first 425 bp of the cassette. After the gentamicin-resistant shuttle vector was generated, a full-length copy of *hk1* plus 325 bp of upstream sequence was amplified with primers Hk1 compl-5′ and Hk1 compl-3′ and cloned into the BamHI and PstI sites of pSP1G. The resulting vector, Hk1-pSP1G, was electrotransformed into Bb1197, and two gentamicin-resistant transformants (Bb1363 and Bb1367) were selected. The presence of the complementing copy of *hk1* was confirmed using primers hk1-KO junc-5′ and hk1-KO-3′; expression of *hk1* in the complemented mutants was confirmed by reverse transcription-PCR (RT-PCR) using cDNAs derived from *in vitro* grown organisms using these same primers.

SDS-PAGE and Western blot analyses. Whole-cell lysates were prepared from spirochetes cultivated either *in vitro* at 23°C and following a temperature shift to 37°C or within DMCs as previously described (11). Equivalent amounts of lysate ($\sim 2 \times 10^7$ spirochetes) were separated through 12.5% separating polyacrylamide mini-gels and visualized by silver staining. For immunoblotting, proteins were transferred to nylon-supported nitrocellulose and incubated with rat polyclonal antiserum directed against FlaB (9), BBA62/Lp6.6 (42), BBA24/DbpA (33), OspE (1), or Rrp1 (58), followed by goat anti-rat secondary antibody (Southern Biotechnology Associates, Birmingham, AL). Blots were developed using the SuperSignal West Pico chemiluminescence substrate (Pierce, Rockford, IL).

Animal infectivity and tick-related studies. To assess infectivity of wild-type and *hk1* mutant strains, 5-to 8-week-old female C3H/HeJ mice (five per group, per isolate) were inoculated intradermally with either 10^4 or 10^3 spirochetes. Infection was assessed at 2 and 4 weeks postinfection by serology and cultivation of tissues in BSK-II medium containing an antibiotic cocktail (0.05 mg/ml sulfamethoxazole, 0.02 mg/ml phosphomycin, 0.05 mg/ml rifampin, 0.01 mg/ml trimethoprim, and 0.0025 mg/ml amphotericin B) to minimize contamination. Cultures were monitored weekly by dark-field microscopy.

To generate naturally infected ticks, approximately 300 to 400 pathogen-free *I. scapularis* larvae (Oklahoma State University, Stillwater, OK) were placed on infected C3H/HeJ mice 2 to 3 weeks after syringe inoculation; the ticks were allowed to feed to repletion and then held in an environmental incubator until they had molted to the nymphal stage. To obtain fed nymphs, 10 to 12 infected flat *I. scapularis* nymphs were confined to a capsule affixed to the backs of naïve C3H/HeJ mice as previously described (49). Unless otherwise indicated, nymphs were allowed to feed until fully engorged. Immersion-fed larvae were generated according to the method described by Policastro and Schwan (56).

All animal experimentation was conducted following the NIH guidelines for housing and care of laboratory animals and was performed in accordance with the University of Connecticut Health Center and University of Maryland institutional regulations after review and approval by Institutional Animal Care and Use Committees at each respective institution.

Quantitative real-time RT-PCR. Total RNA was isolated from infected ticks using TRIzol reagent (Invitrogen) according to the manufacturer's instructions. Contaminating genomic DNA was removed using Turbo DNA*free* (Ambion, Inc., Austin, TX). DNase-treated RNAs (1 to 4 μg of total RNA per sample) were converted to cDNA using SuperScript III (Invitrogen) in the presence and absence of reverse transcriptase (RT) according to the manufacturer's instructions. cDNAs (with RT) were assayed in quadruplicate using iQ Supermix (Bio-Rad). Transcript copy numbers were calculated using the iCycler postrun analysis software based on internal standard curves and then normalized against copies of *flaB*. Normalized copy number values were compared within Prism, version 5.00 (GraphPad Software, San Diego, CA) using an unpaired *t* test with two-tailed *P* values and a 95% confidence interval.

Assessment of *B. burgdorferi* burdens within infected murine tissues. Spirochete burdens within infected murine tissues were assessed at 4 weeks postinfection. Twenty to 80 mg of each tissue was digested with 20× (vol/wt) 0.1% type I collagenase A (Sigma-Aldrich) at 37°C for 4 h and then mixed with an equal volume of 0.2 mg/ml proteinase K in 200 mM NaCl, 20 mM Tris-HCl (pH 8.0), 50 mM EDTA, and 1% sodium dodecyl sulfate. After overnight incubation at 55°C, 200 μl of each digested tissue was mixed with an equal volume of ATL buffer (Qiagen). Subsequent steps were performed using a Qiagen DNeasy blood and tissue kit according to the manufacturer's instructions. TaqMan-based *flaB* (88) and nidogen (81) assays were performed using iQ Supermix (Bio-Rad). Each DNA sample was assayed in quadruplicate, and genome copy numbers were calculated using the CFX Manager (Bio-Rad) postrun analysis software based on internal standard curves. Normalized values were compared within Prism, version 5.00, using an unpaired *t* test with two-tailed *P* values and a 95% confidence interval.

Assessment of *B. burgdorferi* burdens within *I. scapularis* ticks. Spirochete burdens were assessed by quantitative PCR (qPCR) using individual pools of 15 larvae fed to repletion on syringe-inoculated mouse (3 mice per group, per isolate) or triplicate pools of 15 larvae infected by immersion and fed to repletion on a naïve mouse. Total genomic DNA was isolated from surface-sterilized larvae using a Gentra Puregene Yeast and Bacteria kit (Qiagen) according to the manufacturer's instructions. DNAs were diluted 1:10 in water prior to being

assayed for *flaB* as described above. Spirochete viability was assessed by plating on semisolid medium (pBSK) as previously described (60). Plates were monitored for up to 4 weeks for the appearance of colonies. For immunofluorescence, pools of 15 larvae were crushed into 500 μl of ice-cold 1× CMRL medium, centrifuged for 10 min at 4,000 × *g*, washed twice with ice-cold 1× CMRL medium, and resuspended in 40 μl. Aliquots of each suspension (four per pool) were smeared on polylysine-treated slides, and spirochetes were detected using fluorescein isothiocyanate (FITC)-conjugated anti-*Borrelia* antibody (Kirkegaard and Perry Laboratories, Gaithersburg, MD) as previously described (49).

Microinjection of *B. burgdorferi* into naïve *I. scapularis* nymphs and confocal immunofluorescence microscopy. Spirochetes were microinjected into the rectal openings of naïve nymphal ticks as described previously (54, 88). Forty-eight hours after injection, nymphs (15 per mouse) were allowed to feed on naïve C3H/HeN mice. Spirochetes within dissected midguts were detected using FITC-conjugated anti-*Borrelia* antibody, counterstained with propidium iodide, and mounted in antifade reagent for examination. Spirochetes within unfed nymphs were similarly analyzed at 10 days postinjection. Specimens were viewed using an LSM 510 scanning laser confocal microscope equipped with an argon/krypton laser. Images were acquired using a 40× (1.2 numerical aperture [NA]) water immersion objective with 512- by 512-pixel resolution at 1-μm intervals through the full thickness of the sample. Image acquisition and analyses were performed using LSM 5 AIM, version 4.2, software.

Time-lapse epifluorescence imaging of spirochetes within gelatin matrices. The time-lapse imaging studies described here and below require the use spirochetes that constitutively express green fluorescent protein (GFP). We therefore used pMC1389 to inactivate *hk1* within Bb914, a virulent CE162 isolate containing a highly stable P_{flaB}-*gfp* reporter (16); two GFP-positive (GFP^+) *hk1* mutants (Bb1152 and Bb1155) were selected. Gelatin matrices (~1 mm thick) were prepared as previously described (16). Approximately 1×10^8 *in vitro* cultivated spirochetes were added to each chamber well, and slides were incubated for 1 h at room temperature. Each chamber was rinsed twice with sterile phosphate-buffered saline (PBS) before being viewed by epifluorescent microscopy on an Olympus BX41 microscope (Center Valley, PA) using a 40× (1.3 NA) oil immersion objective. Motility was recorded using Streampix high-speed imaging software (Norpix, Canada) at 40 frames per s over 10-s intervals using a Retiga EXi charge-coupled device (CCD) camera (Q Imaging, Canada). A minimum of 200 organisms for each isolate were categorized per experiment. Each isolate was assayed in at least two independent experiments.

RESULTS

The Hk1/Rrp1 phosphorelay scheme involves a previously unrecognized Hpt domain within Hk1. Autophosphorylation and subsequent phosphorelay by HKs typically are mediated by kinase core (DHp and CA domains) (17), REC (28), and histidine-containing phosphotransfer (Hpt) domains (39). Using the NCBI Conserved Domain Database (CDD), we were able to localize kinase core and REC domains within Hk1, but we initially were unable to identify the Hpt domain required for phosphorelay between Hk1 and Rrp1. We confirmed the presence of this requisite domain within the C terminus of Hk1 by multiple sequence alignment with seven prototypical hybrid HKs (see Fig. S1A in the supplemental material). The predicted Hk1 Hpt domain contains three residues, including the active-site histidine (H1252), that are highly conserved across a broad range of Hpt domains (see Fig. S1A) (39, 48). The Hk1 Hpt domain also closely modeled the corresponding domain from a newly described hybrid HK (Protein Data Bank [PDB] code 3MYF; RMSD of 0.1 Å) from *Shewanella* sp. W3-18-1 (see Fig. S1B) and displayed an overall fold that was highly similar to the folds of the well-characterized Hpt domains from BarA (PDB code 3IQT; RMSD of 1.3 Å) and ArcB (PDB code 1FR0; RMSD of 3.2 Å). Identification of this phosphotransfer domain enables us to propose a complete phosphorelay scheme for the Hk1/Rrp1 TCS based on established models for other HKs (39, 84) (see Fig. S1C).

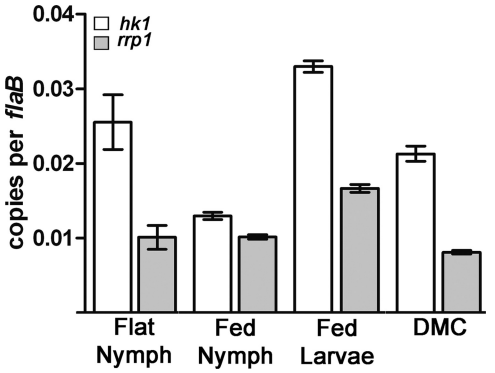

FIG. 1. Expression profiling of *hk1* and *rrp1*. Values represent the average *flaB*-normalized transcript copy number ± standard error of the mean for each gene. Values for *hk1* were significantly different ($P < 0.05$) for the following comparisons: flat nymph versus fed larvae and fed nymph, fed larvae versus fed nymph and DMC, and fed nymph versus DMC. Values for *rrp1* were significantly different ($P < 0.05$) for the following comparisons: fed larvae versus flat nymph, fed nymph and DMC, and DMC versus flat nymph and fed larvae. *hk1* was expressed at significantly ($P < 0.05$) higher levels than *rrp1* in the same sample under all four conditions examined. The sequences of the forward and reverse primers used to detect *hk1* and *rrp1* are provided in Table 2, and their locations are shown in Fig. 2A (hk1-F and hk1-R are designated by arrows 3 and 4, respectively; rrpl-F and rrpl-R are designated by arrows 5 and 6, respectively).

***hk1* and *rrp1* are expressed by *B. burgdorferi* throughout the enzootic cycle.** Expression profiling of *hk1* and *rrp1* was performed to gain insight into the function of this TCS during the enzootic cycle. In preliminary studies, we used semiquantitative RT-PCR across the *hk1-rrp1* intergenic region to confirm that these genes are cotranscribed *in vitro* and within with dialysis membrane chambers (DMCs) (data not shown). We then performed quantitative RT-PCR (qRT-PCR) on RNAs isolated from *I. scapularis* ticks infected with wild-type strain 297 while the mammalian host phase was represented by DMC-cultivated organisms. Overall, both genes were expressed at low levels (~1 to 3 copies per 100 copies of *flaB*). We observed higher levels of *hk1*, the upstream gene, than of *rrp1* under all conditions (Fig. 1), which is not surprising given that the gene length of *hk1* is ~4.5 kb. While both genes were expressed within all tick stages and DMCs, transcript levels were highest in larvae fed to repletion and flat nymphs (Fig. 1). Given prior data demonstrating that the alternate sigma factor RpoS is not expressed within either fed larvae or flat nymphs (11, 49), we postulate that transcription of *hk1* and *rrp1* is controlled by the housekeeping sigma factor, RpoD. Indeed, we identified a putative σ^{70} promoter (TTGCCA-18-TTT AAA) located 77 nucleotides upstream of the Hk1 ATG start codon. Constitutive expression of *hk1* and *rrp1* implies that the corresponding TCS functions at multiple points within the tick-mouse cycle.

Hk1 is not required for mammalian host adaptation. To functionally characterize Hk1, we inactivated *hk1* by insertion of a P_{flgB}-*aadA* cassette conferring resistance to streptomycin in *B. burgdorferi* (Fig. 2A). The point of insertion within Hk1 (Val153) is located within the predicted periplasmic sensor domain, and, as such, the mutant polypeptide would lack both sensing and signal transduction capabilities. Two indepen-

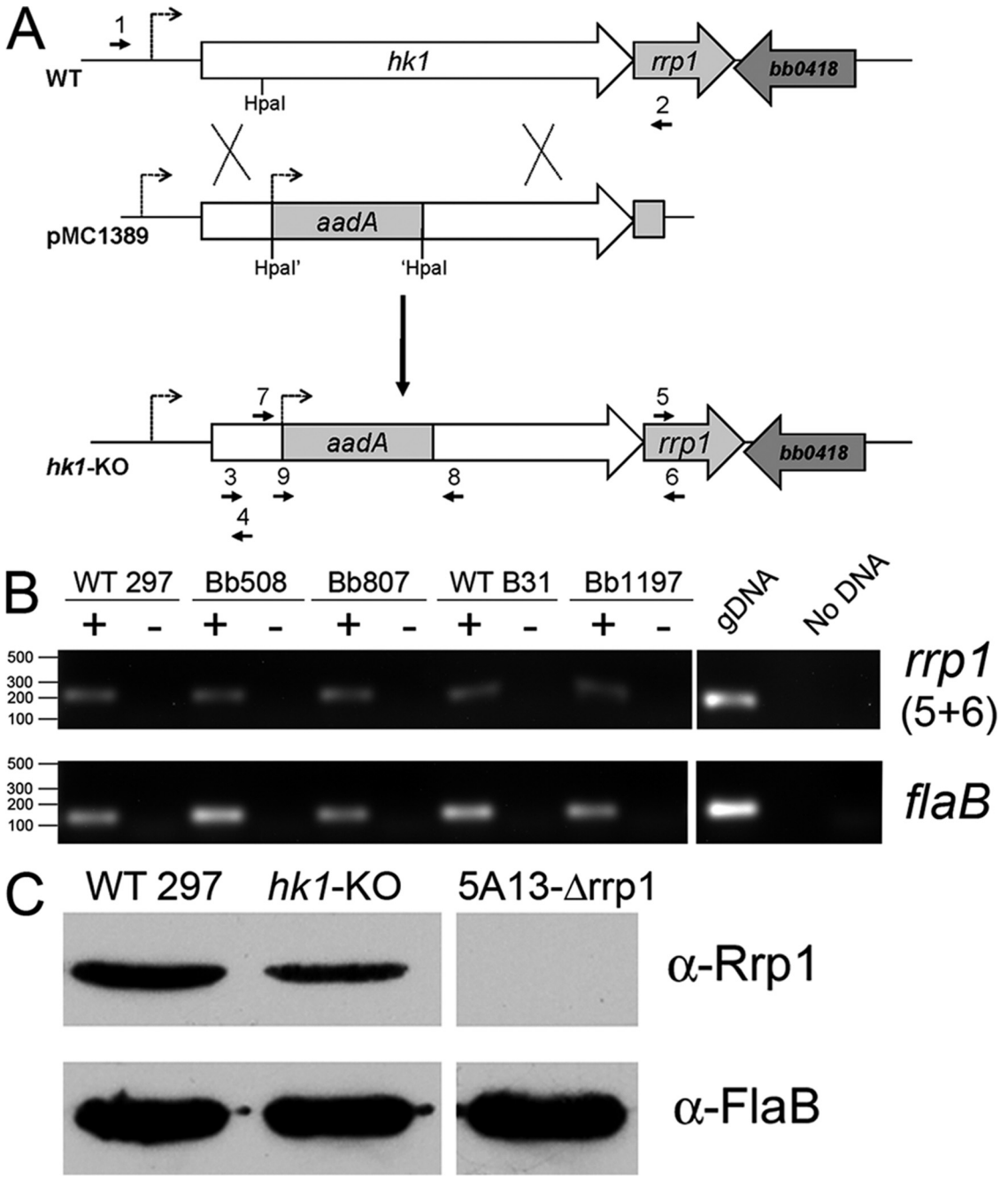

FIG. 2. (A) Strategy for inactivation of *hk1*. The *hk1* coding sequence plus upstream and downstream flanking regions was amplified from strain 297 using primers ups.hk1-5′ and dwns.hk1-3′ (1 and 2). The *hk1* coding sequence was disrupted by insertion of a P_{flgB}-*aadA* antibiotic resistance cassette into an HpaI restriction site present within the endogenous *hk1* gene, yielding pMC1389. Only the relevant portion of pMC1389 is shown. Insertion of the *hk1* KO allele was confirmed in strain 297 and B31 mutant isolates using primers hk1-KO-5′ and hk1-KO-3′ (7 and 8) (see Fig. S2 in the supplemental material). Primer sequences are provided in Table 2. (B) Hk1-deficient spirochetes continue to express Rrp1. Semiquantitative RT-PCR was performed on RNAs isolated from a wild-type (WT) (297 and B31) and *hk1* KO strains (Bb508, Bb807, and Bb1197) using primers specific for *rrp1* (5 and 6) and *flaB*. RT indicates the absence (−) or presence (+) of reverse transcriptase in the reaction mixture. Purified genomic DNA (gDNA) was used as positive controls. (C) Detection of Rrp1 by immunoblotting. Whole-cell lysates of CE162 (WT 297), Bb508 (*hk1*-KO), and a previously characterized B31 5A13 Δ*rrp1* isolate (58) were immunoblotted with rat polyclonal antisera directed against Rrp1 (58) with FlaB used as a loading control. α, anti.

dently derived *hk1* mutants (Bb508 and Bb807) containing full plasmid complements were obtained using our virulent strain 297 isolate CE162 (Table 1). Insertion and orientation of the P_{flgB}-*aadA* cassette were confirmed by PCR (see Fig. S2A in the supplemental material; also data not shown). Both mutants grew identically to their parent at 23°C and 37°C *in vitro* and within DMCs (data not shown). The P_{flgB}-*aadA* cassette used to inactivate *hk1* does not contain a transcriptional terminator

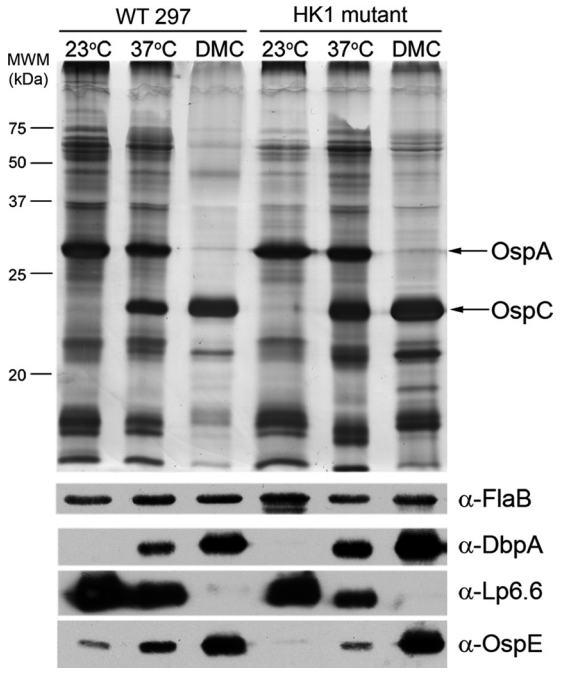

FIG. 3. Hk1 is not required for mammalian host adaptation. Whole-cell lysates from CE162 (WT 297) and Bb508 (Hk1 mutant) were separated by SDS-PAGE, stained with silver, and immunoblotted using antisera directed against DbpA (33), Lp6.6/BBA62 (42), and OspE (1) with FlaB used as a loading control. MWM, molecular weight marker in thousands; α, anti.

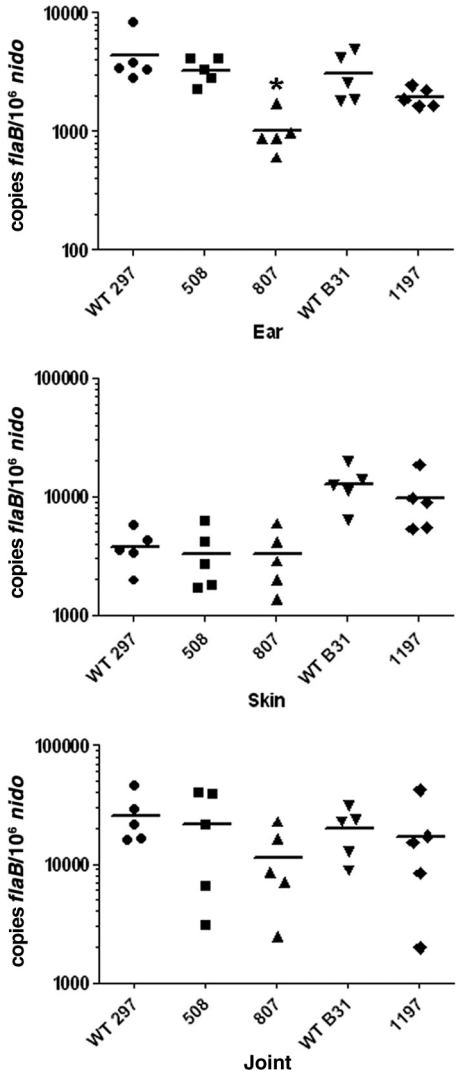

FIG. 4. Spirochetes lacking Hk1 are infectious in mice by syringe inoculation. Tissues were collected from infected mice (5 mice per group) at 4 weeks postinoculation with 10^4 spirochetes of CE162 (WT 297), Bb508, Bb807, B31 5A4 NP1 (WT B31), or Bb1197. Spirochete genome copies, here and elsewhere, were determined using TaqMan assays for spirochetal *flaB* and murine nidogen (*nido*). The mean *nido*-normalized *flaB* value for all mice within a group is indicated by a horizontal line. The asterisk indicates a statistical difference ($P < 0.05$) between CE162 and Bb807 in ear tissue.

and therefore allows for transcriptional read-through and continued expression of *rrp1*. Using RT-PCR and immunoblotting, we first confirmed that our *hk1* mutant isolates continue to express Rrp1 at or near wild-type levels (Fig. 2B and C). We observed few differences between the polypeptide profiles of Bb508 and its parent CE162 following temperature shift *in vitro* and cultivation within DMCs (Fig. 3). The high degree of similarity between the wild-type and mutant DMC proteomes was further substantiated by comparative two-dimensional (2-D) isoelectric focusing (IEF)-SDS-PAGE (data not shown). We also compared the expression profiles of prototypical σ^{70}- and RpoS-dependent lipoproteins associated with mammalian host adaptation and/or virulence (1, 9, 11). Like its parent, Bb508 induced expression of OspC, DbpA, and OspE in response to temperature shift and further enhanced their expression within DMCs (Fig. 3). Moreover, RpoS-mediated repression of OspA and Lp6.6 within DMCs was unaffected by loss of Hk1 (Fig. 3).

***hk1* mutant *B. burgdorferi* organisms are fully virulent in mice but were detected at low levels in larvae following acquisition.** While not required for mammalian host adaptation within DMCs, Hk1 may contribute to other virulence-related aspects of the tick-mouse cycle, such as surface adhesion, dissemination, and/or immune evasion. To test this, we syringe inoculated C3H/HeJ mice (5 per group) with 1×10^4 spirochetes of either *hk1* mutant (Bb508 and Bb807) or of their parent, CE162. At 2 and 4 weeks postinoculation, all mice showed evidence of seroconversion and were culture positive for spirochetes (data not shown). Bb508 also was highly infectious at a dose of 10^3 spirochetes (9/10 mice were culture positive for Bb508 at 4 weeks postinoculation compared to 4/10 mice infected with CE162 at this same dose). We next assessed spirochete burdens within infected tissues at 4 weeks postinoculation by qPCR. With the exception of somewhat lower burdens of Bb807 in ear tissue ($P = 0.012$), we detected comparable numbers of wild-type and *hk1* mutant spirochetes in all tissues examined (Fig. 4). Prior to being sacrificed, these same mice were used to assess whether Hk1 is required for larval acquisition. By qPCR, we observed a >1.5 $\log_{10}$-fold ($P < 0.01$) decrease in the *flaB* copy numbers in larvae fed on mice infected with the *hk1* mutants compared to larvae fed on mice infected with their wild-type counterpart (Fig. 5A). The differ-

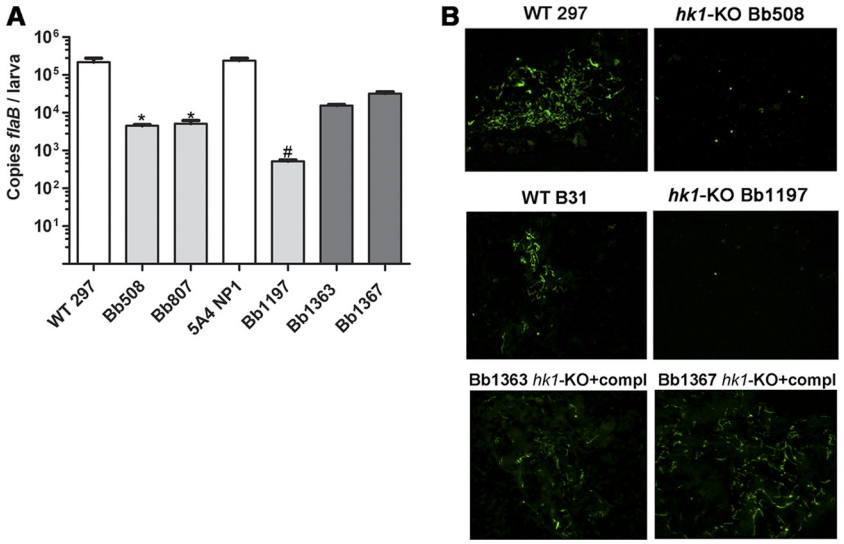

FIG. 5. *hk1* mutants are killed within larvae fed to repletion on syringe-inoculated mice. Data represent spirochete burdens within larvae fed to repletion on C3H/HeJ mice 2 to 3 weeks following syringe inoculation with wild-type parents (CE162 and B31 5A4 NP1), *hk1* mutants (Bb508, Bb807, and Bb1197), or complemented *hk1* mutants (Bb1363 and Bb1367). (A) Spirochete genome copies within pools of 15 larvae collected from individual mice (3 mice per isolate) were determined using a TaqMan assay for *flaB*. Bars represent the mean ± standard error of the mean for each isolate. The normalized *flaB* values for larvae fed on mice infected with *hk1* mutants (*hk1* KO strains) was significantly lower (*, $P = 0.0021$; #, $P < 0.0001$) than that for larvae fed on mice infected with the corresponding parent or complements (compl). (B) Representative micrographs of larvae fed to repletion on syringe-inoculated mice. Pools of 15 larvae from each mouse (3 mice per group) were assessed by IFA using FITC-conjugated anti-*Borrelia* antibody.

ence between the wild-type and mutant burdens was even more pronounced, as determined by plating in pBSK (Table 3) and immunofluorescence assay (IFA) (Fig. 5B); in contrast to the large numbers of viable wild-type spirochetes detected by both methods, few, if any, intact organisms were recovered from or visualized within larvae fed to repletion on mice infected with the *hk1* mutants.

TABLE 3. Semisolid plating of larvae fed to repletion on syringe-inoculated mice

Isolate and group[a]	No. of CFU per larva (avg ± SD)[b]
WT 297	
Larval pool 1	1,395.7 ± 513.4
Larval pool 2	1,629.1 ± 377.3
Larval pool 3	4,650 ± 2,192
Bb508	
Larval pool 1	ND
Larval pool 2	6 ± 6.8
Larval pool 3	ND
Bb807	
Larval pool 1	4.4 ± 3.9
Larval pool 2	0.2 ± 0.4
Larval pool 3	ND
Bb1197	
Larval pool 1	ND
Larval pool 2	ND
Larval pool 3	ND

[a] Strain used to syringe inoculate the mice used for larval infestation.
[b] The number of CFU per larva is based on larvae (15 per pool) fed to repletion on individual infected mice, with 3 mice per isolate (animals M1 to M3). Values represent the average number of CFU (± standard deviation) from three serial dilutions (undiluted, 10^{-1}, and 10^{-2}), plated in duplicate, for each larval pool. ND, no CFU detected.

***B. burgdorferi* spirochetes lacking Hk1 are acquired normally during feeding but are killed within the larval midgut during the blood meal.** The most straightforward interpretation of the above data is that Hk1-deficient spirochetes are being destroyed within the midguts of feeding larvae following acquisition. c-di-GMP has emerged as an important regulator of bacterial virulence (38, 85). Indeed, Sultan et al. (76) recently demonstrated that *B. burgdorferi* lacking BB0363, a c-di-GMP-specific phosphodiesterase, is unable to translate laterally (i.e., reverse their direction of swimming) *in vitro*. The predicted role for Hk1 in activating Rrp1 raised the possibility that the larval acquisition defect displayed by our *hk1* mutants could stem, in part, from their inability to migrate out of the bite site. As a first step toward understanding the contribution of Hk1 to acquisition, we used a gelatin matrix-based assay (16) to compare the motility patterns of wild-type and *hk1* mutant isolates *in vitro*. Although we observed fewer nonmotile *hk1* mutant spirochetes than wild-type organisms (Table 4), these differences were not statistically significant. Moreover, comparable percentages of wild-type and *hk1* mutant organisms could be observed translating laterally within the matrix (Table 4). We next assessed whether Hk1-deficient organisms are acquired normally during feeding. Technical limitations related to the small size and fragile nature of larval midguts required that these timed-feeding studies be performed using naïve nymphs. Previously, Schwan and Piesman (66) demonstrated that spirochetes could be detected within naïve nymphs within 24 h of attachment to an infected mouse. At 24 to 36 h postattachment, we detected comparable numbers of spirochetes in nymphs fed on C3H/HeJ mice infected with either

TABLE 4. *hk1* mutant *B. burgdorferi* display normal motility *in vitro*

Strain	Motility profile (% [mean ± SD])[a]			Total no. of organisms
	Nonmotile	Motile	Translating	
WT 297 (Bb914)	12.67 ± 6.75	87.33 ± 6.74	35.54 ± 8.93	601
hk1 mutant (Bb1152)	4.10 ± 4.55	95.90 ± 4.55	24.42 ± 2.27	465
hk1 mutant (Bb1155)	3.13 ± 2.22	96.88 ± 2.23	30.60 ± 8.10	427

[a] Motility categories are defined as the following: nonmotile, organisms that displayed no discernible signs of motility throughout 10-s imaging interval; motile, organisms that displayed obvious signs of motility at any point during imaging; and translating, organisms within the motile category that also displayed lateral translation in the *x* or *y* axis. Values represent results from at least two independent experiments. A minimum of 200 organisms were scored in each experiment.

wild-type or *hk1* mutant isolates (see Fig. S3 in the supplemental material; also data not shown). Lastly, we artificially infected naïve larvae with CE162, Bb508, and Bb807 by immersion (56), thereby eliminating the migratory aspect of acquisition entirely. Results obtained using immersion-fed larvae were identical to those obtained using larvae fed on syringe-inoculated mice; we observed a marked decrease in the numbers of *hk1* mutant compared to wild-type organisms in fed larvae, as determined by qPCR (Fig. 6A), semisolid plating (Table 5), and IFA (Fig. 6B).

Generation and characterization of a *B. burgdorferi* strain B31 *hk1* mutant and complementation. The dramatic tick phase phenotype displayed by both of our independently derived strain 297 *hk1* mutants is unlikely to be due to a secondary mutation within an unrelated gene(s). Nevertheless, to prove definitively that *hk1* alone is responsible for this phenotype, we attempted to complement both *hk1* mutants with a wild-type copy of *hk1* contained on a shuttle vector. Despite exhaustive efforts, we were unable to transform either Bb508 or Bb807 with this construct. To garner more definitive evi-

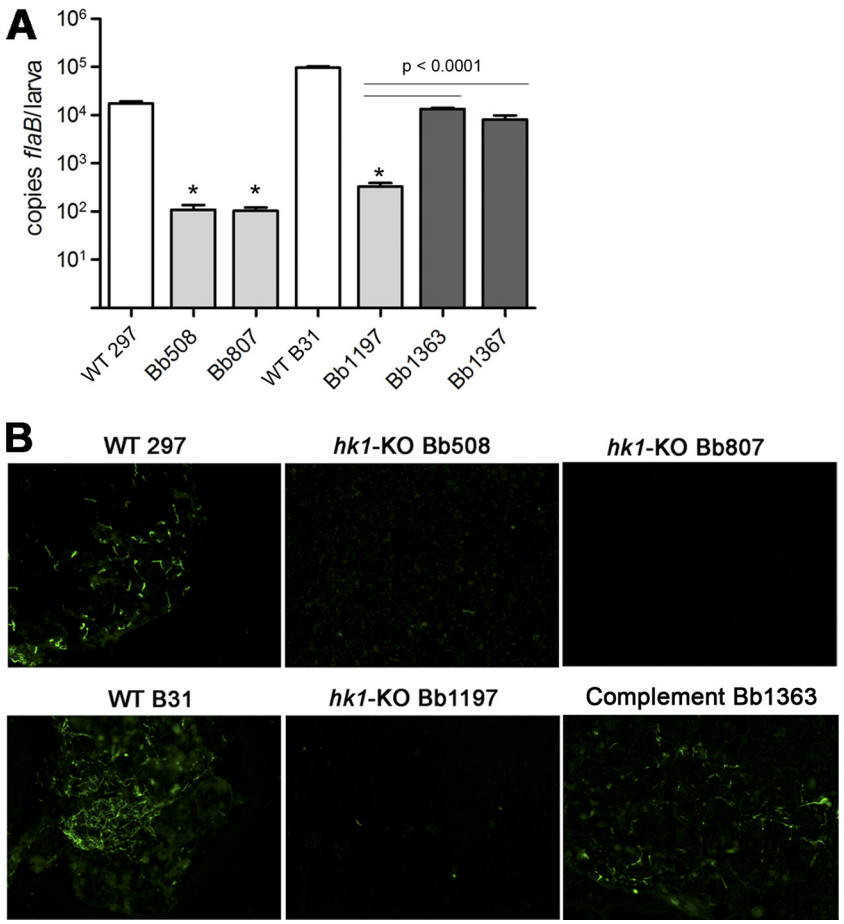

FIG. 6. *hk1* mutants are killed within the midguts of larvae infected by immersion. Larvae infected by immersion with wild-type 297 and B31 (CE162 and 5A4 NP1), *hk1*-KO mutants (Bb508, Bb807 and Bb1197), or complement (Bb1363) were fed to repletion on naïve mice. (A) Spirochete genome copies within triplicate pools of 15 fed larvae. Bars represent the mean *flaB* values per larva ± standard error of the mean for each isolate. Asterisks indicate significantly ($P < 0.0001$) lower values for *hk1* mutants than for the corresponding parent. (B) Representative immunofluorescence micrographs of fed larvae infected by immersion. Pools of 15 fed larvae infected with each strain were assessed by IFA using FITC-conjugated anti-*Borrelia* antibody.

TABLE 5. Semisolid plating of replete larvae infected by immersion

Isolate[a]	No. of CFU per larva (avg ± SD)[b]
WT 297	227.3 ± 94.4
Bb508	0.1 ± 1.3
Bb807	0.3 ± 0.5
WT B31	1,226 ± 855
Bb1197	9.0 ± 9.0

[a] Strain used to immerse naïve larvae. Viability of spirochetes within immersion-fed larvae was assessed after ticks had fed to repletion on naïve mice.

[b] The number of CFU is based on pools of 15 larvae per isolate. Values represent results from three serial dilutions (undiluted, 10^{-1}, and 10^{-2}), plated in triplicate, for each larval pool.

dence that the observed phenotype is due to loss of *hk1*, we inactivated *hk1* in the highly transformable, virulent B31 isolate 5A4 NP1 (40) using the same strategy as used for strain 297, yielding Bb1197 (Table 1). Like its strain 297 mutant counterparts, Bb1197 expressed normal levels of *rrp1* (Fig. 2B), was fully virulent in mice by syringe inoculation (Fig. 4), and was acquired by nymphs during the first 24 h of feeding (see Fig. S3 in the supplemental material). Equally important, Bb1197 was highly sensitive to killing by the larval blood meal (Fig. 5 and 6; Tables 3 and 5). Unlike our strain 297 *hk1* mutants, we obtained multiple complemented isolates using Bb1197 (Table 1; see also Fig. S2C). Using two independent isolates (Bb1363 and Bb1367), we confirmed that survival of Hk1-deficient spirochetes within fed larvae could be restored by *trans*-complementation with a wild-type copy of *hk1* contained on a cp9-based shuttle vector (Fig. 5 to 7 and data not shown).

***hk1* mutant *B. burgdorferi* organisms are killed within nymphal as well as larval midguts.** Our studies thus far have focused on the contribution of Hk1 to survival within feeding larvae. We reasoned, however, that the protection afforded by Hk1 during acquisition also would be required during the nymphal blood meal. But because *hk1* mutants are eliminated from the midguts of fed larvae, we could not assess the role of this gene product within nymphs following the molt. To circumvent this limitation, we used the microinjection technique developed by Pal et al. (53) to administer spirochetes directly into the midguts of naïve nymphs via the rectal opening. Up to 10 days postinjection, we detected similar numbers of wild-type (CE162 and 5A4 NP1) and *hk1* mutant (Bb508, Bb807 and Bb1197) spirochetes within unfed nymphal midguts (Fig. 7 and data not shown), indicating that Hk1 is not required when the midgut epithelium is quiescent. As early as 36 h postattachment, on the other hand, we saw a dramatic decrease in the burdens of all three *hk1* mutants in fed versus unfed midguts (Fig. 7 and data not shown). The numbers of wild-type organisms, in contrast, remained relatively unchanged in response to early feeding (Fig. 7). Survival of spirochetes lacking Hk1 was restored in feeding nymphs by *trans*-complementation (Fig. 7 and data not shown).

The Hk1 sensor domain contains two distinct regions with homology to different amino acid substrate-binding proteins. The molecule(s) responsible for activating the Hk1 sensor domain must be able to traverse the spirochete's outer membrane. We performed detailed *in silico* analyses of this region as a first step toward identifying potential ligands. CDD searches revealed that Hk1's periplasmic sensor consists of two discrete solute-binding domains, designated D1 and D2, both belonging to the Pfam PF00497 family of bacterial extracellular solute-binding proteins. This highly diverse family is typically associated with substrate-binding proteins (SBPs) of ABC-type transporters (47, 78) but recently has been expanded to include a number of sensor histidine kinases (5). Based on homology searches using the Swiss-Model server (2), D1 modeled most closely with ArtJ (PDB 2Q2A; E value of 8.10e−34), an arginine-, lysine-, histidine-binding protein from *Geobacillus stearothermophilus* (82) (see Fig. S4A in the supplemental material), while D2 best matched GlnBP (PDB 1WDN; E value of 1.00e−22), a glutamine-binding protein from *Escherichia coli* (77) (see Fig. S4B). The structural models for D1 and D2 each display features common to ABC transporter- and sensor-type SBPs, namely, two mixed α/β-fold globular lobes connected by a flexible hinge region with a predicted binding pocket located

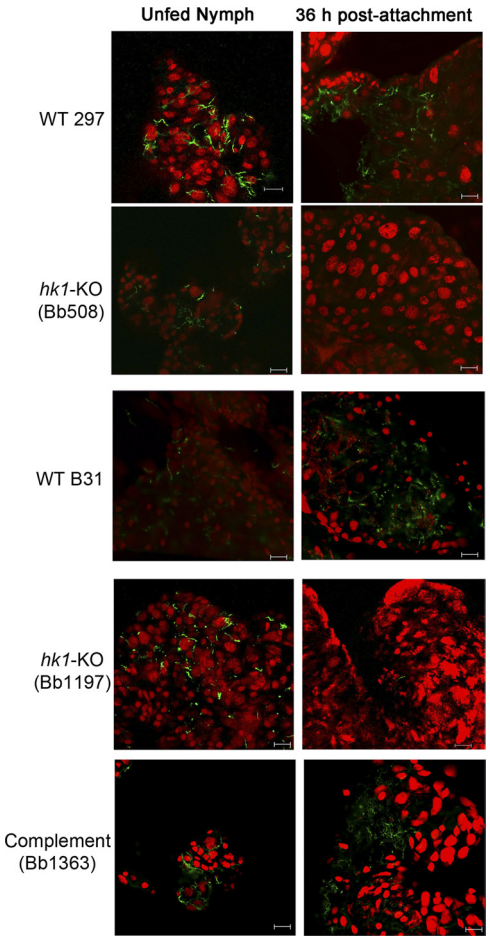

FIG. 7. Hk1 is required for survival within fed but not flat nymphal midguts. Composite confocal image showing the distribution of spirochetes within nymphs infected by rectal microinjection with CE162 (WT 297), Bb807 (*hk1*-KO mutant), Bb1197 (*hk1*-KO mutant), 5A4 NP1 (WT B31), or complement (Bb1363). Spirochetes were detected within midguts carefully dissected from unfed and fed nymphs, forcibly removed at 36 h postattachment, using FITC-conjugated anti-*Borrelia* antibody. The tick midgut was counterstained with propidium iodide (red). Scale bar, 20 μm.

at the interface between the two lobes in each domain (5). Nonsynonymous amino acid substitutions within the predicted binding pockets for D1 and D2 compared to ArtJ and GlnBP (see Fig. S4A and B), respectively, imply that the ligands recognized by D1 and D2 differ from those of their respective structural homolog.

DISCUSSION

Maintenance of *B. burgdorferi* within its enzootic cycle depends upon the spirochete's ability to sense and respond to environmental stimuli encountered within the arthropod vector and mammalian host. Signals contained within the nymphal blood meal trigger a complex series of transcriptional, antigenic, and physiological changes that enable spirochetes colonizing the midgut to disseminate through tick tissues while preparing for growth within the mammalian host (11, 15, 16, 67); the Rrp2/RpoN/RpoS regulatory pathway is central to this transmission-associated program (6, 7, 11, 15, 20, 52, 86, 87). The signaling pathways underlying the converse process, whereby spirochetes transit from the mammalian host into naïve *I. scapularis* ticks, have received comparatively little attention. Here, we demonstrate that the hybrid histidine kinase Hk1 is required for *B. burgdorferi* to survive within the fed midgut environment. Recently, studies by two independent laboratories demonstrated that spirochetes lacking Rrp1 display an identical survival defect (33a, 41a), thereby confirming that the protective function of Hk1 is mediated via phosphorelay. Importantly, spirochetes lacking Hk1 survive for prolonged periods within the midguts of unfed nymphs but are destroyed at the onset of the nymphal blood meal, indicating that the adaptive response mediated by Hk1 is not tick stage specific. Thus, in contrast to the Rrp2/RpoN/RpoS pathway, which functions exclusively during nymphal transmission and subsequent mammalian infection (7, 10, 11, 49, 86), the Hk1/Rrp1 TCS functions during both acquisition and transmission.

Inactivation of *hk1* had no effect on the ability of spirochetes to adapt to the host, disseminate within mice following syringe inoculation, or establish murine infection. Indeed, despite being present at wild-type levels within skin, *hk1* mutant spirochetes were not recovered from larvae fed on syringe-inoculated mice. One can envision two non-mutually exclusive explanations for this defect: (i) *hk1* mutants are unable to exit the feeding site, or (ii) spirochetes lacking Hk1 are being killed following acquisition. Multiple lines of evidence argue in favor of the latter. First, using a gelatin matrix-based assay (16), we determined that loss of Hk1 had no discernible effect on motility; this finding is particularly noteworthy in light of the established link between c-di-GMP and motility in other bacteria (13, 85) and a report by Sultan et al. (76), demonstrating that the manipulation of c-di-GMP levels in *B. burgdorferi* engenders a motility defect *in vitro*. Second, *hk1* mutant organisms could be visualized within the midguts of naïve nymphs at ≤24 h postattachment during the so-called preparatory phase that precedes the ingress of blood and differentiation of midgut epithelial cells (3). Third, we detected appreciable amounts of borrelial genomic DNA by qPCR but scant viable or intact organisms by semisolid plating and IFA, respectively, in larvae fed on *hk1* mutant-infected mice. Lastly, using immersion feeding to circumvent infected mice as a means of introducing *hk1* mutants into naïve larvae, we observed a similar stark difference between spirochete burdens detected by qPCR and the numbers of live and intact organisms detected by plating and IFA.

While further experimentation will be required to establish a definitive biochemical link between Hk1 and Rrp1, the similar phenotypes displayed by our *hk1* mutants and those lacking Rrp1 (33a, 41a) provide compelling evidence that these proteins work cooperatively to promote the synthesis of c-di-GMP. Typically, c-di-GMP exerts its regulatory effects by binding to a wide range of effector molecules, altering either transcription or enzymatic activity (34, 65). In the case of *B. burgdorferi*, the time frame for activation of the Hk1/Rrp1 TCS is more than sufficient to encompass both transcription and *de novo* synthesis of borrelial gene products. We envision two types of adaptive responses that could be initiated within ticks. First, activation of Hk1 may be required for spirochetes to evade killing by noxious substances generated during digestion of the blood meal and/or elaborated by the midgut epithelium (21, 50, 74). Based on the near-complete destruction of Hk1-deficient organisms within fed ticks, we hypothesize that the initial lesion is likely a breach in the spirochete's fragile outer membrane that exposes the underlying cell envelope (4, 8, 43). Our observation that prolonged incubation of *hk1* mutants with 72-h-fed nymphal midguts *ex vivo* did not replicate the killing observed within feeding nymphs (data not shown) implies that killing requires proximity to the midgut epithelium. Spirochetes maintain extensive and prolonged contact with the midgut epithelium within feeding ticks (16), suggesting that the protection afforded by Hk1 extends beyond the early feeding time point in which we observed destruction of our *hk1* mutants. Alternatively, c-di-GMP may regulate borrelial gene products involved in metabolic adaptation to the fed midgut. Along these lines, two independent microarray studies have shown that Rrp1 promotes the transcription of *glp* genes (*bb0240-bb0243*) involved in glycerol uptake and utilization (58; also He et al., submitted); in addition to its role in membrane biogenesis, glycerol is thought to be the principal carbon/energy source for spirochetes within feeding ticks (55; also He et al., submitted). However, constitutive expression of the *glp* operon in spirochetes lacking Rrp1 only partially alleviates the survival defect within engorged ticks (He et al., submitted), implicating additional gene products as part of a larger Hk1/Rrp1-mediated response. In both of the above scenarios, one would predict that Hk1 would be required during the nymphal as well as larval blood meal. We confirmed this supposition by demonstrating that *hk1* mutants survive for prolonged periods in unfed nymphal midguts infected by microinjection but are destroyed as early as 36 h postattachment to a naïve host.

Our working model, presented in Fig. 8, proposes that the periplasmic portion of Hk1 senses host- and/or tick-derived molecules generated during feeding. Tick saliva contains a plethora of bioactive molecules (22, 63, 72). Destruction of host tissues during creation of the feeding lesion and the ensuing inflammatory response would also give rise to nu-

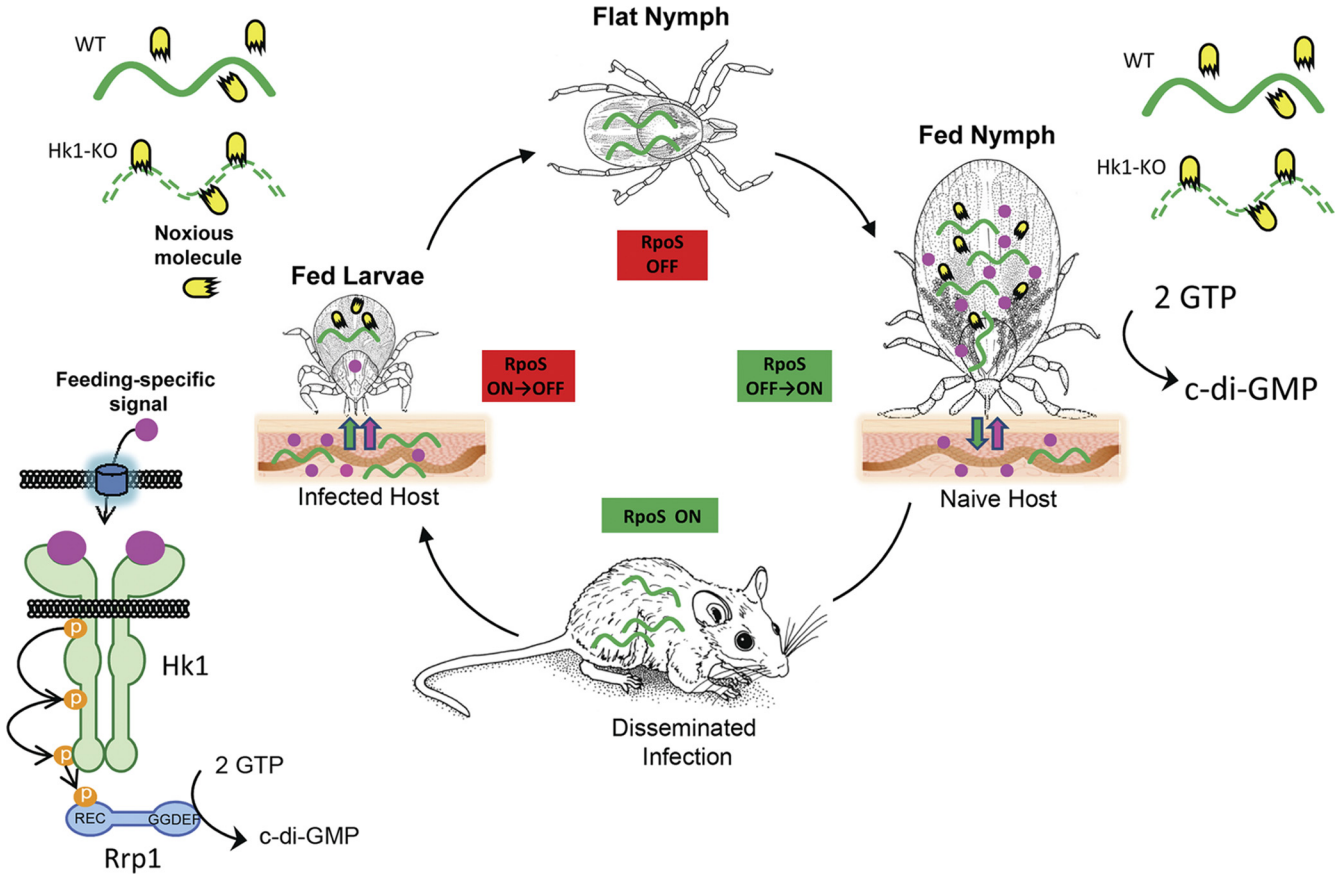

FIG. 8. Working model for Hk1/Rrp1 and Rrp2/RpoN/RpoS TCS during the enzootic cycle. At the onset of feeding, Hk1 senses unique host- and/or tick-derived molecules generated within the feeding site. These feeding-specific molecules must be small enough to rapidly traverse the spirochete's outer membrane and engage Hk1's D1 and D2 periplasmic sensor domains. During acquisition, spirochetes first encounter these molecules as they migrate into the feeding site, while spirochetes within flat nymphs (or larvae infected by immersion) would encounter these ligands solely within the midgut (3). The Hk1/Rrp1-directed synthesis of c-di-GMP initiates an adaptive response that enables spirochetes either to evade killing by noxious substances within midgut epithelium as feeding progresses (21, 37, 50, 73, 74) or to adjust metabolically to growth within the arthropod vector. In contrast to the Rrp2/RpoN/RpoS pathway, which is active (ON) only within feeding nymphs, the Hk1/Rrp1 TCS is essential for survival during both the larval and nymphal blood meals.

merous small molecules (e.g., histamine and serotonin) with signaling potential (46, 61). Thus, the bite site represents an extraordinarily rich milieu for generating ligands able to rapidly traverse the spirochete's outer membrane and engage one or both of the D1 and D2 sensor domains of Hk1. Based on *in silico* structural modeling, we predict that D1 and D2 recognize amino acids (or their derivatives). Interestingly, Scheckelhoff et al. (64) demonstrated that the administration of the β-adrenergic antagonist propranolol to infected mice significantly reduced spirochete burdens within fed larvae; their findings implicate catecholamines, which are derivatives of phenylalanine and tyrosine and plentiful in tick saliva (62), as attractive candidate signaling molecules for Hk1. The requirement for Hk1 at the onset of the nymphal blood meal, on the other hand, implies that signaling molecule(s) involved in activating this sensor histidine kinase also are present within the midgut early during feeding, either imbibed from the bite site as part of the blood meal or elaborated by the differentiating midgut epithelium.

Sensor-type SBPs, such D1 and D2, have emerged as a new structural class of HKs that are thought to function by analogy to the classic "Venus flytrap" model for ABC transporters (12, 35). With transporter SBPs, occupancy of the binding pocket favors a closed conformation, allowing the protein to interact specifically with its cognate permease (19). Ligand binding by sensor SBPs, in contrast, is thought to stabilize an open conformation (12, 35), with the resulting piston-like conformational change stimulating the autophosphorylation of a conserved histidine (predicted to be H773 in Hk1) within the cytoplasmic kinase core (see Fig. S1 in the supplemental material) (29). In a recent study, Herrou et al. (35) proposed that BvgS, a prototype for this new class of HKs, is constitutively active in the unbound (i.e., closed) state and is deactivated by ligand binding. This scenario seems unlikely for Hk1 because phosphorylation of Rrp1 is a prerequisite for diguanylate cyclase activity (59). While the presence of tandem SBPs is common among periplasmic histidine kinase sensor domains (Microbial Signal Transduction Database; Agile Genomics, Mount Pleasant, SC), little is known regarding whether these domains function cooperatively. One intriguing possibility is that D1

and D2 recognize signaling molecules that are unique to the acquisition and transmission phases of the enzootic cycle and function independently to promote activation of Hk1 within feeding larvae and nymphs.

The data in this paper, together with other studies (9, 11, 15, 20, 49, 52, 70, 86), allow us to contrast the Hk1/Rrp1 and Hk2/Rrp2 regulatory pathways while, at the same time, envisioning how these two TCSs may collaborate to promote the maintenance of *B. burgdorferi* in nature (Fig. 8). The Rrp2/RpoN/RpoS pathway is induced during the nymphal blood meal and presumably stays ON throughout infection, transitioning from an ON to OFF state during larval acquisition (11, 49). The apparent lack of cross talk between the spirochete's two TCSs is consistent with the intrinsic ability of HKs to recognize their cognate response regulator to the exclusion of all others (69). The role of Hk2 as the principle means of activating Rrp2 was unexpectedly called into question by Xu et al. (86), who demonstrated that phosphorylation of Rrp2 also can be mediated via the high-energy phosphate donor acetyl~P. The dramatic phenotype associated with loss of Hk1 within feeding nymphs indicates that acetyl~P is unable to promote phosphorylation of Rrp1, thereby creating a definitive barrier between these two signal transduction pathways. That the Hk1/Rrp1 is ON during the larval and nymphal blood meals is strong evidence not only that the Hk1/Rrp1 and Rrp2/RpoN/RpoS pathways are activated by disparate environmental stimuli but also that the physiological cues that promote activation of Rrp2 are specific to the nymphal blood meal. Despite their strict segregation, the Hk1/Rrp1 and Rrp2/RpoN/RpoS regulatory pathways are, nevertheless, clearly interdependent. The most obvious example is the protective function of Hk1/Rrp1, without which spirochetes could not be transmitted by feeding nymphs. While destruction of spirochetes lacking either Hk1 or Rrp1 (33a, 41a) precludes a direct examination of the transcriptional changes elicited by this TCS during tick feeding, microarray analyses performed using *in vitro* cultivated organisms indicate that Rrp1 and, by extension, c-di-GMP, move the spirochete's transcriptional set point toward the expression of tick phase genes (58). Thus, it is tempting to speculate that "pressure" from the Hk1/Rrp1 TCS drives the transition from an RpoS-ON to RpoS-OFF state during acquisition and delays the downregulation of tick phase genes until spirochetes have been successfully transmitted to the mammalian host. Regarding the latter, we have shown that downregulation of tick phase genes, such as *ospA*, is RpoS dependent but occurs slowly over the course of the nymphal blood meal (9, 11, 49), while Ohnishi et al. (51) elegantly documented that many spirochetes continue to express OspA within the feeding site. We hypothesize that mammalian host adaption is not complete until spirochetes have migrated away from the bite site and are no longer subject to the regulatory effects of c-di-GMP.

ACKNOWLEDGMENTS

We thank Anna Allard for her technical assistance and Meghan Lybecker for her efforts regarding the transformation of strain 297 *hk1* mutant isolates. We are indebted to Daniel Sonenshine for this many helpful suggestions and advice on the tick physiology.

This work was supported in part by NIH/NIAID grants AI-29735 and 3R01AI029735-20S1 (J.D.R. and M.J.C.), AI085248 (M.J.C.), A1080615 (U.P.), and AI059373 and AI085310 (D.R.A.), along with grants from the Oklahoma Center for the Advancement of Science and Technology (HR09-002 to D.R.A.), the National Research Fund for Tick-Borne Diseases (M.J.C.), and a New England Regional Center of Excellence Fellowship (U54 AI-057159 to S.D.-E.).

REFERENCES

1. **Akins, D. R., K. W. Bourell, M. J. Caimano, M. V. Norgard, and J. D. Radolf.** 1998. A new animal model for studying Lyme disease spirochetes in a mammalian host-adapted state. J. Clin. Invest. **101:**2240–2250.
2. **Arnold, K., L. Bordoli, J. Kopp, and T. Schwede.** 2006. The SWISS-MODEL workspace: a web-based environment for protein structure homology modelling. Bioinformatics **22:**195–201.
3. **Balashov, Y. S.** 1972. Blood-sucking ticks (Ixodidae)-vectors of disease of man and animals. Misc. Pub. Entomol. Soc. Am. **8:**161–376.
4. **Bergstrom, S., and W. R. Zuckert.** 2010. Structure, function and biogenesis of the *Borrelia* cell envelope, p. 139–166. *In* D. S. Samuels and J. D. Radolf (ed.), *Borrelia*: molecular biology, host interaction and pathogenesis. Calister Academic Press, Norfolk, United Kingdom.
5. **Berntsson, R. P. A., S. H. J. Smits, L. Schmitt, D.-J. Slotboom, and B. Poolman.** 2010. A structural classification of substrate-binding proteins. FEBS Lett. **584:**2606–2617.
6. **Blevins, J. S., et al.** 2009. Rrp2, a σ^{54}-dependent transcriptional activator of *Borrelia burgdorferi*, activates *rpoS* in an enhancer-independent manner. J. Bacteriol. **191:**2902–2905.
7. **Boardman, B. K., et al.** 2008. Essential role of the response regulator Rrp2 in the infectious cycle of *Borrelia burgdorferi*. Infect. Immun. **76:**3844–3853.
8. **Boylan, J. A., K. A. Lawrence, J. S. Downey, and F. C. Gherardini.** 2008. *Borrelia burgdorferi* membranes are the primary targets of reactive oxygen species. Mol. Microbiol. **68:**786–799.
9. **Caimano, M. J., C. H. Eggers, C. A. Gonzalez, and J. D. Radolf.** 2005. Alternate sigma factor RpoS is required for the *in vivo*-specific repression of *Borrelia burgdorferi* plasmid lp54-borne *ospA* and *lp6.6* genes. J. Bacteriol. **187:**7845–7852.
10. **Caimano, M. J., C. H. Eggers, K. R. Hazlett, and J. D. Radolf.** 2004. RpoS is not central to the general stress response in *Borrelia burgdorferi* but does control expression of one or more essential virulence determinants. Infect. Immun. **72:**6433–6445.
11. **Caimano, M. J., et al.** 2007. Analysis of the RpoS regulon in *Borrelia burgdorferi* in response to mammalian host signals provides insight into RpoS function during the enzootic cycle. Mol. Microbiol. **65:**1193–1217.
12. **Cheung, J., M. Le-Khac, and W. A. Hendrickson.** 2009. Crystal structure of a histidine kinase sensor domain with similarity to periplasmic binding proteins. Proteins **77:**235–241.
13. **Cotter, P. A., and S. Stibitz.** 2007. c-di-GMP-mediated regulation of virulence and biofilm formation. Curr. Opin. Microbiol. **10:**17–23.
14. **DeLano, W. L.** 2002. The PyMOL molecular graphics system. DeLano Scientific, San Carlos, CA.
15. **de Silva, A. M., K. R. Tyson, and U. Pal.** 2009. Molecular characterization of the tick-*Borrelia* interface. Front. Biosci. **14:**3051–3063.
16. **Dunham-Ems, S. M., et al.** 2009. Live imaging reveals a novel, biphasic mode of dissemination of *Borrelia burgdorferi* within ticks. J. Clin. Invest. **119:**3652–3665.
17. **Dutta, R., L. Qin, and M. Inouye.** 1999. Histidine kinases: diversity of domain organization. Mol. Microbiol. **34:**633–640.
18. **Eggers, C. H., et al.** 2002. Identification of loci critical for replication and compatibility of a *Borrelia burgdorferi* cp32 plasmid and use of a cp32-based shuttle vector for the expression of fluorescent reporters in the Lyme disease spirochaete. Mol. Microbiol. **43:**281–295.
19. **Felder, C. B., R. C. Graul, A. Y. Lee, H.-P. Merkle, and W. Sadee.** 1999. The Venus flytrap of periplasmic binding proteins: an ancient protein module present in multiple drug receptors. AAPS Pharm. Sci. **1:**1–20.
20. **Fisher, M. A., et al.** 2005. *Borrelia burgdorferi* σ^{54} is required for mammalian infection and vector transmission but not for tick colonization. Proc. Natl. Acad. Sci. U. S. A. **102:**5162–5167.
21. **Fogaça, A. C., et al.** 1999. Antimicrobial activity of a bovine hemoglobin fragment in the tick *Boophilus microplus*. J. Biol. Chem. **274:**25330–25334.
22. **Francischetti, I. M., A. Sa-Nunes, B. J. Mans, I. M. Santos, and J. M. Ribeiro.** 2009. The role of saliva in tick feeding. Front. Biosci. **14:**2051–2088.
23. **Frank, K. L., S. F. Bundle, M. E. Kresge, C. H. Eggers, and D. S. Samuels.** 2003. *aadA* confers streptomycin resistance in *Borrelia burgdorferi*. J. Bacteriol. **185:**6723–6727.
24. **Fraser, C. M., et al.** 1997. Genomic sequence of a Lyme disease spirochaete, *Borrelia burgdorferi*. Nature **390:**580–586.
25. **Galperin, M.** 2005. A census of membrane-bound and intracellular signal transduction proteins in bacteria: bacterial IQ, extroverts and introverts. BMC Microbiol. **5:**35.
26. **Galperin, M. Y.** 2010. Diversity of structure and function of response regulator output domains. Curr. Opin. Microbiol. **13:**150–159.
27. **Galperin, M. Y., A. N. Nikolskaya, and E. V. Koonin.** 2001. Novel domains

of the prokaryotic two-component signal transduction systems. FEMS Microbiol. Lett. **203:**11–21.
28. **Gao, R., T. R. Mack, and A. M. Stock.** 2007. Bacterial response regulators: versatile regulatory strategies from common domains. Trends Biochem. Sci. **32:**225–234.
29. **Gao, R., and A. M. Stock.** 2009. Biological insights from structures of two-component proteins. Annu. Rev. Microbiol. **63:**133–154.
30. **Gilmore, R. D., et al.** 2010. The *bba64* gene of *Borrelia burgdorferi*, the Lyme disease agent, is critical for mammalian infection via tick bite transmission. Proc. Natl. Acad. Sci. U. S. A. **107:**7515–7520.
31. **Goldstein, S. F., et al.** 2010. The chic motility and chemotaxis of *Borrelia burgdorferi*, p. 167–188. *In* D. S. Samuels and J. D. Radolf (ed.), *Borrelia*: molecular biology, host interaction, and pathogenesis. Caister Academic Press, Norfolk, United Kingdom.
32. **Grimm, D., et al.** 2004. Outer-surface protein C of the Lyme disease spirochete: A protein induced in ticks for infection of mammals. Proc. Natl. Acad. Sci. U. S. A. **101:**3142–3147.
33. **Hagman, K. E., et al.** 1998. Decorin-binding protein of *Borrelia burgdorferi* is encoded within a two-gene operon and is protective in the murine model of Lyme borreliosis. Infect. Immun. **66:**2674–2683.
33a. **He, M., et al.** 2011. Cyclic di-GMP is essential for the survival of the Lyme disease spirochete in ticks. PLoS Pathog. **7:**e1002133.
34. **Hengge, R.** 2009. Principles of c-di-GMP signalling in bacteria. Nat. Rev. Microbiol. **7:**263–273.
35. **Herrou, J., et al.** 2010. Periplasmic domain of the sensor-kinase BvgS reveals a new paradigm for the Venus flytrap mechanism. Proc. Natl. Acad. Sci. U. S. A. **107:**17351–17355.
36. **Hubner, A., et al.** 2001. Expression of *Borrelia burgdorferi* OspC and DbpA is controlled by a RpoN-RpoS regulatory pathway. Proc. Natl. Acad. Sci. U. S. A. **98:**12724–12729.
37. **Hynes, W. L., S. M. Ceraul, S. M. Todd, K. C. Seguin, and D. E. Sonenshine.** 2005. A defensin-like gene expressed in the black-legged tick, *Ixodes scapularis*. Med. Vet. Entomol. **19:**339–344.
38. **Jenal, U., and J. Malone.** 2006. Mechanisms of cyclic-di-GMP signaling in bacteria. Annu. Rev. Genet. **40:**385–407.
39. **Kato, M., T. Mizuno, T. Shimizu, and T. Hakoshima.** 1997. Insights into multistep phosphorelay from the crystal structure of the C-terminal Hpt domain of ArcB. Cell **88:**717–723.
40. **Kawabata, H., S. J. Norris, and H. Watanabe.** 2004. BBE02 disruption mutants of *Borrelia burgdorferi* B31 have a highly transformable, infectious phenotype. Infect. Immun. **72:**7147–7154.
41. **Kenedy, M. R., S. R. Vuppala, C. Siegel, P. Kraiczy, and D. R. Akins.** 2009. CspA-mediated binding of human factor H inhibits complement deposition and confers serum resistance in *Borrelia burgdorferi*. Infect. Immun. **77:**2773–2782.
41a. **Kostick, J. L., et al.** 2011. The diguanylate cyclase, Rrp1, regulates critical steps in the enzootic cycle of the Lyme disease spirochetes. Mol. Microbiol. doi:10.1111/j.1365-2958.2011.07687.x.
42. **Lahdenne, P., et al.** 1997. Molecular characterization of a 6.6-kilodalton *Borrelia burgdorferi* outer membrane-associated lipoprotein (lp6.6) which appears to be downregulated during mammalian infection. Infect. Immun. **65:**412–421.
43. **LaRocca, T. J., et al.** 2010. Cholesterol lipids of *Borrelia burgdorferi* form lipid rafts and are required for the bactericidal activity of a complement-independent antibody. Cell Host Microbe **8:**331–342.
44. **Laub, M. T.** 2010. The role of two-component signal transduction systems in bacterial stress responses, p. 45–58. *In* G. Storz and R. Hengge (ed.), Bacterial stress responses, 2nd ed. ASM Press, Washington, DC.
45. **Lee, E. R., J. L. Baker, Z. Weinberg, N. Sudarsan, and R. R. Breaker.** 2010. An allosteric self-splicing ribozyme triggered by a bacterial second messenger. Science **329:**845–848.
46. **Mans, B. J., et al.** 2008. Comparative sialomics between hard and soft ticks: implications for the evolution of blood-feeding behavior. Insect Biochem. Mol. Biol. **38:**42–58.
47. **Mascher, T., J. D. Helmann, and G. Unden.** 2006. Stimulus perception in bacterial signal-transducing histidine kinases. Microbiol. Mol. Biol. Rev. **70:**910–938.
48. **Matsushika, A., and T. Mizuno.** 1998. The structure and function of the histidine-containing phosphotransfer (Hpt) signaling domain of the *Escherichia coli* ArcB sensor. J. Biochem. **124:**440–445.
49. **Mulay, V. B., et al.** 2009. *Borrelia burgdorferi bba74* is expressed exclusively during tick feeding and is regulated by both arthropod- and mammalian host-specific signals. J. Bacteriol. **191:**2783–2794.
50. **Nakajima, Y., D. Taylor, and M. Yamakawa.** 2002. Involvement of antibacterial peptide defensin in tick midgut defense. Exp. Appl. Acarol. **28:**135–140.
51. **Ohnishi, J., J. Piesman, and A. M. de Silva.** 2001. Antigenic and genetic heterogeneity of *Borrelia burgdorferi* populations transmitted by ticks. Proc. Natl. Acad. Sci. U. S. A. **98:**670–675.
52. **Ouyang, Z., J. S. Blevins, and M. V. Norgard.** 2008. Transcriptional interplay among the regulators Rrp2, RpoN and RpoS in *Borrelia burgdorferi*. Microbiology **154:**2641–2658.
53. **Pal, U., et al.** 2004. TROSPA, an *Ixodes scapularis* receptor for *Borrelia burgdorferi*. Cell **119:**457–468.
54. **Pal, U., et al.** 2004. OspC facilitates *Borrelia burgdorferi* invasion of *Ixodes scapularis* salivary glands. J. Clin. Invest. **113:**220–230.
55. **Pappas, C. J., et al.** 2011. *Borrelia burgdorferi* requires glycerol for maximum fitness during the tick phase of the enzootic cycle. PLoS Pathog. **7:**e1002102.
56. **Policastro, P. F., and T. G. Schwan.** 2003. Experimental infection of *Ixodes scapularis* larvae (Acari: Ixodidae) by immersion in low passage cultures of *Borrelia burgdorferi*. J. Med. Entomol. **40:**364–370.
57. **Pollack, R. J., S. R. Telford, and A. Spielman.** 1993. Standardization of medium for culturing Lyme disease spirochetes. J. Clin. Microbiol. **31:**1251–1255.
58. **Rogers, E. A., et al.** 2009. Rrp1, a cyclic-di-GMP-producing response regulator, is an important regulator of *Borrelia burgdorferi* core cellular functions. Mol. Microbiol. **71:**1551–1573.
59. **Ryjenkov, D. A., M. Tarutina, O. V. Moskvin, and M. Gomelsky.** 2005. Cyclic diguanylate is a ubiquitous signaling molecule in bacteria: insights into biochemistry of the GGDEF protein domain. J. Bacteriol. **187:**1792–1798.
60. **Samuels, D. S.** 1995. Electrotransformation of the spirochete *Borrelia burgdorferi*. Electrotransformation protocols for microorgansims. Methods Mol. Biol. **47:**253–259.
61. **Sangamnatdej, S., G. C. Paesen, M. Slovak, and P. A. Nuttall.** 2002. A high affinity serotonin- and histamine-binding lipocalin from tick saliva. Insect Mol. Biol. **11:**79–86.
62. **Sauer, J. R., R. C. Essenberg, and A. S. Bowman.** 2000. Salivary glands in ixodid ticks: control and mechanism of secretion. J. Insect Physiol. **46:**1069–1078.
63. **Sauer, J. R., J. L. McSwain, A. S. Bowman, and R. C. Essenberg.** 1995. Tick salivary gland physiology. Annu. Rev. Entomol. **40:**245–267.
64. **Scheckelhoff, M. R., S. R. Telford, M. Wesley, and L. T. Hu.** 2007. *Borrelia burgdorferi* intercepts host hormonal signals to regulate expression of outer surface protein A. Proc. Natl. Acad. Sci. U. S. A. **104:**7247–7252.
65. **Schirmer, T., and U. Jenal.** 2009. Structural and mechanistic determinants of c-di-GMP signalling. Nat. Rev. Microbiol. **7:**724–735.
66. **Schwan, T. G., and J. Piesman.** 2000. Temporal changes in outer surface proteins A and C of the Lyme disease-associated spirochete, Borrelia burgdorferi, during the chain of infection in ticks and mice. J. Clin. Microbiol. **38:**382–388.
67. **Schwan, T. G., J. Piesman, W. T. Golde, M. C. Dolan, and P. A. Rosa.** 1995. Induction of an outer surface protein on *Borrelia burgdorferi* during tick feeding. Proc. Natl. Acad. Sci. U. S. A. **92:**2909–2913.
68. **Seshu, J., et al.** 2006. Inactivation of the fibronectin-binding adhesin gene *bbk32* significantly attenuates the infectivity potential of *Borrelia burgdorferi*. Mol. Microbiol. **59:**1591–1601.
69. **Skerker, J. M., et al.** 2008. Rewiring the specificity of two-component signal transduction systems. Cell **133:**1043–1054.
70. **Smith, A. H., J. S. Blevins, G. N. Bachlani, X. F. Yang, and M. V. Norgard.** 2007. Evidence that RpoS (σ^S) in *Borrelia burgdorferi* is controlled directly by RpoN (σ^{54}/σ^N). J. Bacteriol. **189:**2139–2144.
71. **Smith, K. D., et al.** 2009. Structural basis of ligand binding by a c-di-GMP riboswitch. Nat. Struct. Mol. Biol. **16:**1218–1223.
72. **Sonenshine, D. E.** 1993. Biology of the ticks. Oxford University Press, New York, NY.
73. **Sonenshine, D. E., S. M. Ceraul, W. E. Hynes, K. R. Macaluso, and A. F. Azad.** 2002. Expression of defensin-like peptides in tick hemolymph and midgut in response to challenge with *Borrelia burgdorferi*, *Escherichia coli* and *Bacillus subtilis*. Exp. Appl. Acarol. **28:**127–134.
74. **Sonenshine, D. E., and W. L. Hynes.** 2008. Molecular characterization and related aspects of the innate immune response in ticks. Front. Biosci. **13:**7046–7063.
75. **Stewart, P. E., R. Thalken, J. L. Bono, and P. Rosa.** 2001. Isolation of a circular plasmid region sufficient for autonomous replication and transformation of infectious *Borrelia burgdorferi*. Mol. Microbiol. **39:**714–721.
76. **Sultan, S. Z., J. E. Pitzer, M. R. Miller, and M. A. Motaleb.** 2010. Analysis of a *Borrelia burgdorferi* phosphodiesterase demonstrates a role for cyclic-di-guanosine monophoase in motility and virulence. Mol. Microbiol. **77:**128–142.
77. **Sun, Y. J., J. Rose, B. C. Wang, and C. D. Hsiao.** 1998. The structure of glutamine-binding protein complexed with glutamine at 1.94 Å resolution: comparison with other amino acid binding proteins. J. Mol. Biol. **278:**219–229.
78. **Tam, R., and M. H. Saier, Jr.** 1993. Structural, functional, and evolutionary relationships among extracellular solute-binding receptors of bacteria. Microbiol. Rev. **57:**320–346.
79. **Thompson, J. D., D. G. Higgins, and T. J. Gibson.** 1994. Clustal W: improving the sensitivity of progressive multiple sequence alignment through weighting positions-specific gap penalties and weight matrix choice. Nucleic Acids Res. **22:**4673–4680.
80. **Tilly, K., A. Bestor, M. W. Jewett, and P. Rosa.** 2007. Rapid clearance of Lyme disease spirochetes lacking OspC from skin. Infect. Immun. **75:**1517–1519.
81. **Tupin, E., et al.** 2008. NKT cells prevent chronic joint inflammation after

infection with *Borrelia burgdorferi*. Proc. Natl. Acad. Sci. U. S. A. **105:**19863–19868.
82. **Vahedi-Faridi, A., et al.** 2007. Crystal structures and mutational analysis of the arginine-, lysine, and histidine-binding protein ArtJ from *Geobacillus stearothermophilus*. Implications for interactions of ArtJ with its cognate ATP-binding cassette transporter, $Art(MP)_2$. J. Mol. Biol. **375:**448–459.
83. **Weening, E. H., et al.** 2008. *Borrelia burgdorferi* lacking *dbpBA* exhibits an early survival defect during experimental infection. Infect. Immun. **76:**5694–5705.
84. **West, A. H., and A. M. Stock.** 2001. Histidine kinases and response regulator proteins in two-component signaling systems. Trends Biochem. Sci. **26:**369–376.
85. **Wolfe, A. J., and K. L. Visick.** 2008. Get the message out: cyclic-di-GMP regulates multiple levels of flagellum-based motility. J. Bacteriol. **190:**463–475.
86. **Xu, H., et al.** 2010. Role of acetyl-phosphate in activation of the Rrp2-RpoN-RpoS pathway in *Borrelia burgdorferi*, p. PLoS Pathog. **6:**piie1001104.
87. **Yang, X. F., S. M. Alani, and M. V. Norgard.** 2003. The response regulator Rrp2 is essential for the expression of major membrane lipoproteins in *Borrelia burgdorferi*. Proc. Natl. Acad. Sci. U. S. A. **100:**11001–11006.
88. **Yang, X. F., U. Pal, S. M. Alani, E. Fikrig, and M. V. Norgard.** 2004. Essential role for OspA/B in the life cycle of the Lyme disease spirochete. J. Exp. Med. **199:**641–648.

Editor: A. Camilli